Published in final edited form as:
J Immunol. 2012 March 15; 188(6): 2866–2875. doi:10.4049/jimmunol.1103461.

Significant role of IL-1 signaling, but limited role of inflammasome activation in oviduct pathology during *Chlamydia muridarum* genital infection[1]

Uma M. Nagarajan[*,†,2], **James D. Sikes**[†], **Laxmi Yeruva**[†], and **Daniel Prantner**[*,3]

[*]Department of Microbiology and Immunology, University of Arkansas for Medical Sciences, and Arkansas Children's Hospital Research Institute, Little Rock, AR 72202

[†]Department of Pediatrics, University of Arkansas for Medical Sciences, and Arkansas Children's Hospital Research Institute, Little Rock, AR 72202

Abstract

IL-1β has been implicated in the development of oviduct pathology during *Chlamydia muridarum* genital infection in the mouse model. The goal of this study was to characterize the role of IL-1 signaling and the inflammasome activation pathways during genital chlamydial infection. Compared to control mice, IL-1R-deficient mice displayed delayed clearance and increased chlamydial colonization. Consistent with the role for IL-1 signaling in infection clearance, mice deficient for IL-1R antagonist cleared infection at a faster rate. Despite increased infection, IL-1R deficient mice had significantly reduced oviduct pathology, which was associated with decreased numbers of neutrophils but more macrophages in the genital tract. IL-1β secretion is dependent on caspase-1 and ASC inflammasome during in vitro infection of primed macrophages with *C. muridarum*. To investigate the role of inflammasome components during in vivo genital infection, mice lacking NLRP3, NLRC4, and ASC were tested and found to display no reduction in oviduct pathology compared to control mice. Mice deficient for ASC displayed a prolonged course of infection, which was associated with reduced T cell recruitment and proliferation. Further, ASC-deficient mice displayed normal levels of IL-1β levels in genital secretions. However a significant decrease in caspase-1-dependent IL-18 was observed in both ASC and NLRP3 deficient mice. These data demonstrate a major role for IL-1 signaling but a limited role for inflammasome pathway in IL-1β secretion and development of oviduct pathology during genital chlamydial infection. The data also suggests an IL-1-independent role for ASC in adaptive immunity during genital chlamydial infection.

[1]The project described was supported by Grant Number AI067678 (NIAID) to U.N. and in part, by the Arkansas Children's Hospital Research Institute and the Arkansas Biosciences Institute.

[2]Address correspondence to: Uma M. Nagarajan, Ph.D. Division of Pediatric Infectious Diseases, Arkansas Children's Hospital Research Institute, 13 Children's Way, Room 2052, Little Rock, AR 72202, Tel: (501) 364-2479, Fax: (501) 364-2403, nagarajanuma@uams.edu.

[3]**Present address** – Department of Microbiology and Immunology, University of Maryland School of Medicine, Baltimore, MD 21201

[4]**Abbreviations used in this paper:** AIM2, absent in melanoma2; ASC, apoptosis associated speck-like protein containing CARD domain; CARD, caspase recruitment domain; IFU, inclusion forming units; KO, knockout; NLR, NOD-like receptor; NOD1, nucleotide-binding oligomerization domain 1; T3S, type III secretion; WT, wild type.

Introduction

Chlamydia trachomatis is currently the most common bacterial sexually transmitted infection in the world. *C. trachomatis* infection in women has been identified as an important public health problem due to the negative impact on female reproduction secondary to scarring of the fallopian tubes [reviewed in (1)]. The female mouse genital tract infection model using *C. muridarum* has been invaluable in dissecting the elements that contribute to upper genital tract pathology following infection. Using this model, it has been shown that inflammatory cytokines induced following TLR2 stimulation are major players in development of oviduct pathology during genital *C. muridarum* infection (2).

We have previously shown that IL-1β KO mice develop significantly less oviduct pathology during *C. muridarum* infection (3), suggesting that downstream signaling by IL-1β during chlamydial infection could be the mechanistic basis for this phenotype. IL-1α and IL-1β exert a similar biological function by binding to the IL-1 receptor 1 (IL-1R), a member of a large family of interleukin receptors and triggering downstream effects including induction of proinflammatory cytokines [reviewed in (4)]. Conversely, IL-1Ra is a natural antagonist of IL-1α and IL-1β, preventing uncontrolled immune activation by IL-1α/β through competitive binding to IL-1R (5). During chlamydial infection, IL-1β is produced in large amounts by infiltrating macrophages and neutrophils (3), suggesting that it is a primary cytokine in downstream IL-1R activation. IL-1β is initially expressed in its pro-form and only converted to a biologically active form following proteolytic cleavage by the protease caspase-1(6, 7). Caspase-1 KO mice infected with *C. muridarum* exhibit less pathology in the mouse oviducts in comparison to wild type controls (8), suggesting that activation of the cysteine protease caspase-1 is important for the development of host pathology.

Due to the integral inflammatory function of IL-1β, caspase-1 activation is controlled in a rigorous manner. Caspase-1 is activated in the cytosol in a multiprotein scaffold termed the inflammasome (9), which forms only in response to different danger signals including bacterial or viral infections (10-13). Multiple cytosolic Nod-like receptor (NLR) proteins function as the upstream sensor proteins in this pathway. Currently, there are four defined inflammasomes; all of which contain procaspase-1 and the crucial adaptor molecule “apoptosis associated speck-like protein containing CARD domain” or ASC (14), which bridges procaspase-1 to the NLR sensor proteins (15). Inflammasomes are classified by the unique NLR protein present in conjunction with these two common protein components. NLRP3 triggers activation in response to many stimuli including extracellular ATP, large insoluble structures, and pore forming toxins (13, 16, 17). NLRC4 is able to recognize a conserved molecular motif present in both bacterial flagellin and also many bacterial rod proteins that are found in the bacterial Type III secretion apparatus (18-20). Nalp1b activates caspase-1 in response to *Bacillus anthracis* lethal toxin (21). The most recently identified inflammasome is AIM2, which is able to sense cytosolic dsDNA (18, 22, 23)

The entire development cycle of *C. muridarum* occurs in an intracellular compartment named the inclusion, and it is intriguing how cytosolic pathways are able to interact with *C. muridarum* during infection in order to activate caspase-1. Two studies using RNAi techniques to knockdown expression of inflammasome components in HeLa and THP-1

cells showed that NLRP3 and ASC are necessary for activation of caspase-1 during chlamydial infection (24, 25). Using macrophages from mice deficient for inflammasome components, a similar dependence for IL-1β secretion on NLRP3 and ASC but not NLRC4 was observed during *Chlamydia pneumoniae* infection (26). However, it is not known whether the same components are involved in inflammasome activation and IL-1β secretion during in vivo genital infection and how they influence infection clearance and disease outcome. In this study we extend our results from IL-1β KO mice (3) and confirm the important role of IL-1 signaling for infection clearance and its detrimental role for oviduct pathology. Further, we investigated how these results relate to inflammasome activation during genital *C. muridarum* infection. In vitro infection of prestimulated macrophages results in IL-1β secretion in an ASC-dependent, but NLRP3-independent manner suggesting multiple pathways for inflammasome activation. However, during in vivo infection, IL-1β secretion was predominantly ASC-independent. As a consequence, mice deficient for inflammasome components develop oviduct pathology comparable to wild type (WT) mice, unlike IL-1R-deficient mice. In addition, a significant role for ASC in T cell response and infection clearance was uncovered.

Materials and Methods

Chlamydial stocks

Chlamydia muridarum, "Nigg" strain, was propagated in *Mycoplasma*-free McCoy cells grown in DMEM media supplemented with 100 μM nonessential amino acids (Invitrogen), 2 mM L-glutamine (Invitrogen), 10% FBS, 50 mg/ml gentamicin sulfate (Gemini Bioproducts), and 0.5 mg/ml cycloheximide. Infectious elementary bodies were isolated at 30 h postinfection by first scraping the plates with a cell scraper followed by sonication for 1 min with a sonic dismembrator with a probe attachment (Fisher Scientific). The resulting cell extracts were spun at 300 g for 5 min, and the pellet containing any remaining cellular debris was discarded. Supernatants were spun down at 30,960 g/16,000 rpm for 30 min at 4°C in a Beckman Coulter Avanti J-25 centrifuge fixed with a 25.50 JA rotor. Chlamydial bodies were washed, spun a second time in PBS, and resuspended in SPG buffer (250 mM sucrose, 10 mM sodium phosphate, and 5 mM L-glutamic acid, pH 7.2) in small volume aliquots (∼50 ml), and finally stored at −80°C. The infectious titer of the stock was determined by infecting a fresh McCoy cell monolayer and calculating Inclusion Forming Units (IFUs) as described below.

Mouse strains

Mice deficient for IL-1R1 subunit (IL-1R KO, Stock No. 003245) and mice deficient for IL-1 receptor antagonist (IL-1Ra KO, Stock No. 004754) were purchased from the Jackson Laboratory. Mice deficient for inflammasome components; NLRP3 KO, NLRC4 KO, and ASC KO mice (all in C57BL/6 background) were kind gifts from Genentech Inc. (PI: Dr. Vishva Dixit) (13, 27). All control mice used in this study for in vivo infection or macrophage isolation were C57BL/6J mice (Stock # 000664) Jackson Laboratory, Bar Harbor, ME). All animal experiments were approved by the Institutional Animal Care and Use Committee at the University of Arkansas for Medical Sciences.

Genital infections of mice

Seven days prior to infection, each mouse received 2.5 mg of Depo-Provera subcutaneously in 100 μl of PBS. A week later, mice were anesthetized with Nembutal (200-230 μl of 1:10 PBS diluted stock) and infected by administering 1×10^6 infectious forming units of *C. muridarum* in 10 μl SPG buffer (250 mM sucrose, 10 mM sodium phosphate, 5 mM L-glutamate) directly into the vaginal vault.

Specimen collection from in vivo infections

Chlamydial colonization was determined by swabbing the cervix and vaginal vault of infected mice with a calcium alginate swab (Spectrum Medical Instruments, Los Angeles, CA) at various times postinfection. IFUs were calculated as described below. Additionally, genital secretions were collected one day prior to infection (d0) and also throughout the duration of infection and processed for cytokine analysis. Briefly, mice were anesthetized with Nembutal and absorbent sponges were placed into the vagina for 30 min. Sponges were removed and stored at −80°C until further processing. At that time, cytokines were then eluted from the sponges with PBS containing 0.5% BSA, and 0.05% Tween-20 using Spin-X centrifuge tubes (Fisher Scientific #07-200-385). Sponges were placed in the upper chamber of these tubes in 350 μl of the elution solution and vortexed vigorously for 1 min. Elution was allowed to occur on ice for a further 1 h. Finally, after vortexing again for 1 min, samples were spun in a tabletop centrifuge at 9,300 g for 5 min at 4°C.

Histopathology

Genital tract tissues were extracted enbloc from mice sacrificed on day 45 postinfection. Tissues were fixed in 10% buffered formalin and embedded in paraffin. Longitudinal sections (4 μm) were stained with hematoxylin and eosin and evaluated by a pathologist blind to the experimental design. Each anatomic site (exocervix, endocervix, uterine horn, oviduct, and mesosalpinx) was assessed independently for the presence of neutrophils, mononuclear cells (lymphocytes and monocytes), plasma cells, and fibrosis. Right and left uterine horns and right and left oviducts were evaluated individually. A four–tiered, semi-quantitative scoring system was used to quantitate the inflammation and fibrosis: 0 = normal; 1+ = rare foci (minimal presence) of parameter; 2+ = scattered (1-4) aggregates or mild diffuse increase in parameter; 3+ = numerous aggregates (>4) or moderate diffuse or confluent areas of parameter; 4+ = severe diffuse infiltration or confluence of parameter. Luminal distention of the uterine horns, granulomas, and dilatation of the oviducts were graded from 1 to 4, with grade 4 representing peak severity or frequency of the parameter.

Cytokine quantification

The protein levels of IL-1β in genital secretions and culture supernatants were determined using either an ELISA kit (SMLB00C, R&D Systems) (supernatants) or a MilliplexR Map mouse cytokine/chemokine kit (Cat. No. MPXMCYTO-70K-04). For ELISA analysis of IL-1β, eluates were diluted 1:20 prior to the assay. IL-18 and IFNγ were analyzed directly from the eluates by ELISA using kits from MBL (Cat. No. 7625) and R&D systems (Cat. No. MIF00), respectively. Optical densities taken at 450 nm for quantification were measured using a Biotek plate reader.

Inclusion Forming Unit (IFU) determination

IFUs were calculated by reinfecting a fresh McCoy cell monolayer in 96-well black plates. Cells were fixed at 24 h postinfection with methanol. Inclusions were visualized by staining cells using anti-*C. muridarum* mouse immune sera (1:300 dilution) followed by Alexa fluor 488 conjugated anti mouse IgG (1:1,000 dilution in PBS) (Southern Biotechnology) with 0.1% Evans blue solution as a counter stain. Inclusions were counted using an Olympus fluorescent microscope to calculate the IFU/ml of each sample. For each sample assayed, the numbers of inclusions in 5 to 20 fields were counted. The IFU/ml was calculated by multiplying the total number of inclusions by the dilution factor, the field factor (20/# fields counted), and the scalar 42.33.

Macrophage isolation and in vitro infection

Peritoneal macrophages were obtained and cultured as described (28) for in vitro infections. All infections were performed in antibiotic-free media on cells that were allowed to rest in culture at least 48 hours following isolation from the mouse. Alternately, some macrophages were frozen (DMEM, 35% FBS, 10% DMSO) and stored in liquid nitrogen until needed and treated upon thawing as above. *C. muridarum* was added at 1 multiplicity of infection (MOI) to cells in tissue culture plates. Next, cells were centrifuged at 1,690 g at 37°C for 1 h. The media was replaced with fresh complete media. To confirm the cells were infected, macrophages in wells containing coverslips were fixed with methanol for 10 min at room temperature at 24 h postinfection and stained with the FITC conjugated Pathfinder anti-chlamydial monoclonal antibody (Bio-Rad). Prestimulation of macrophages with *E.coli* LPS at 100 ng/ml was carried out 6 h before infection as described earlier (3).

T cell proliferation

On day 14 postinfection, all mice were sacrificed and iliac lymph nodes were harvested, macerated through a 70-μm mesh filter and brought into single cell suspension. The cells were resuspended at 2.5×10^6/ml, and 100 μl of each suspension was added to 100 μl of media, or media containing 5 μg/ml ConA, or 5 μg/ml chlamydial antigen. Chlamydial antigen was prepared by isolating *C. muridarum* EBs from infected HeLa cells by renograffin centrifugation (29). The EBs were UV inactivated and tested for lack of viability prior to use in assays. Each treatment was assayed in at least triplicate. After 96 hours of incubation, 20 μl of supernatants per well were pulled and replaced with 20 μl alamarBlue™ (Invitrogen). Fluorescence was read on a 96-well Biotek plate reader.

Flow cytometric analysis of genital tract cells from infected mice

Cervical tissue, uterine horns, and both oviducts were excised from the genital tract of an individual mouse, minced, and incubated separately with 1 ml of collagenase I (SIGMA #C0130) (1 mg/ml) for 20 min at 37°C. After neutralizing the enzymes with EDTA (10 μM), 100 μl of cell suspension was diluted with equal volume of SPG buffer and frozen at -70°C until IFU determination on McCoy plate, as described earlier. Remaining cells were passed through a mesh filter (70 μm) using DMEM with 0.5% FBS. Cell suspension were centrifuged and resuspended in 1 ml of FACS buffer (PBS, 1% BSA, and 1 mM EDTA) and passed through filter top tubes (BD # 352235). Cells ($2\text{-}5 \times 10^5$ cells/25 μl) were incubated

in Fc-Block (5 μg/ml) for 10 min, followed by staining for individual cell surface markers or isotype controls (5 μg/ml) in a 96-well V bottom plate for 20 min on ice. The following mAbs (BD Biosciences) were used: CD45 PerCP Cy5.5 (clone 30-11), Ly6G-FITC (clone IA8), F4/80-APC (clone BMB), and CD4-PE (clone RM-4). Cells were washed with FACS buffer and resuspended with 200 μl of FACS buffer containing DAPI (500 ng/ml). Cells were analyzed immediately after staining using FACS Aria (BD BioScience) and the resulting data analyzed using Flo-Jo software (Tree star Inc.).

Statistical analysis

Where indicated, at least three independent experiments were performed in order to test for significance using SigmaStat (Systat Software Inc.). For more than two treatment groups, a one-way ANOVA with pairwise multiple comparison (Holm-Sidak method) was performed to determine statistically significant differences. Statistical comparison between the two mouse strains for IFU quantification or cytokine analysis over the course of infection were made by a 2-way ANOVA with the post-hoc Tukey test as a multiple comparison procedure. The Fisher-exact test was used for determination of significant differences in the frequency of hydrosalpinx observed in the two groups. For analysis of pathology scores, Kruskal-Wallis one-way ANOVA on ranks was performed. One-way ANOVA or unpaired student T test was used for determining significance between individual groups in flow cytometry data.

Results

IL-1R signaling is essential for optimal clearance of genital chlamydial infection, but plays a detrimental role in oviduct pathology

We have previously shown that IL-1β KO mice displayed an enhanced colonization and delayed clearance of *C. muridarum* infection in comparison to WT mice (3). To further address the function of IL-1 signaling, the infection course of *C. muridarum* in the genital tract was studied using IL-1R KO mice. IL-1R KO mice showed significantly enhanced levels of chlamydial colonization and delayed clearance of infection in the genital tract in comparison to WT mice (Fig 1A and B). Consistent with the observed role for IL-1 signaling in controlling infection, mice deficient for IL-1 antagonist (IL-1Ra KO), which show increased IL-1 response (30), showed reduced bacterial colonization and earlier clearance of infection compared to WT mice (Fig 1C and D).

At day 45 postinfection, mice were sacrificed for assessment of gross pathology and histopathological observations. IL-1R KO mice showed significantly reduced incidence of oviduct hydrosalpinx (HS) ($p<0.0001$) (Fig 2A). Histopathological observation of the oviduct showed significantly reduced dilation in IL-1R KO mice compared to WT mice, but no differences in acute (PMN), chronic (mononuclear cells) and plasma cells, between the two groups at this terminal time point (Fig 2B and C). However, the uterine horns showed significantly more dilation and numbers of chronic and plasma cells (data not shown), which could relate to the delayed infection clearance in these mice. Contrary to the IL-1R KO mice, IL-1Ra KO mice showed an increase in the incidence of oviduct pathology in comparison to WT (Total oviducts with HS: WT= 15/30, IL-1Ra KO 13/20; mice with HS:

WT=10/15, IL-1Ra KO=9/10), but this difference was not statistically significant (Fig 2D). Histopathological observation of IL-1Ra KO oviducts showed significantly increased numbers of acute, chronic, and plasma cells (Fig 2E and F), suggesting increased inflammation, despite early infection clearance (Fig 1C).

IL-1β secretion from macrophages infected with *C. muridarum* is partially dependent on ASC

IL-1β is one of the predominant cytokine in the genital secretion during *C. muridarum* infection and is primarily produced by macrophages and neutrophils (3). Considering its abundance and importance, it is hypothesized to be the major player in IL-1 signaling. To initially determine how IL-1β secretion is regulated by inflammasome components during *C. muridarum* infection, in vitro infections were performed in macrophages obtained from WT, ASC KO, NLRP3 KO, and NLRC4 KO mice. In LPS-primed macrophages, ATP-induced IL-1β secretion depended on both ASC and NLRP3 but not NLRC4 (Fig 3A), as has been previously shown (13). However, IL-1β secretion in LPS-primed macrophages following infection with *C. muridarum* was independent of NLRP3 and NLRC4 but dependent on ASC (Fig 3B). Pro-IL-1β mRNA expression following prestimulation with *E. coli* LPS was not impaired in ASC KO (data not shown), implying that the decreased IL-1β secretion is due to lack of caspase-1 activation. Since NLRP3 has been implicated in activation of caspase-1 following chlamydial infection of unprimed cells (25), these experiments were also performed with unstimulated macrophages. With no prestimulation, macrophages secrete lower levels of IL-1β than LPS-primed macrophages upon *C. muridarum* infection. Interestingly, unlike prestimulated macrophages, IL-1β secretion from unstimulated macrophages infected with *C. muridarum* was completely dependent on ASC and NLRP3 (Fig 3C). Pro-IL-1β mRNA expression levels in infected macrophages were similar between WT, ASC KO and NLRP3 KO macrophages (data not shown). Overall, these data suggest that in addition to NLRP3, *C. muridarum* activates an inflammasome that contains both ASC and a pyrin domain containing NLR protein, but not NLRC4, during in vitro infection of presstimulated macrophages.

ASC is required for optimal clearance of *C. muridarum* from the female genital tract

We have hypothesized that during in vivo infection, macrophages and neutrophils coming to the site of infection can get prestimulated by various chlamydial TLR ligands (3). To investigate the role of inflammasome components in IL-1β secretion and its relationship to infection clearance and oviduct pathology, ASC KO, NLRP3 KO, NLRC4 KO, and WT mice were infected genitally with *C. muridarum*. ASC KO mice exhibited increased bacterial colonization and prolonged courses of infection in comparison to WT mice (Fig 4A). NLRP3 KO mice also showed slightly increased chlamydial colonization and a delay in infection clearance, although the differences were not statistically significant in multiple experiments compared to WT mice (Fig 4B). Conversely, NLRC4 KO mice showed no differences in the rate of chlamydial clearance or colonization (Fig 4C). To further establish the levels of bacterial colonization, genital tract tissues derived from mice from an independent study were processed for chlamydial IFU at day 10 postinfection. ASC KO mice showed a significant increase in chlamydial IFU, while NLRP3 and NLRC4 KO mice showed a marginal increase which was not statistically significant (data not shown).

At day 45 postinfection, the mice were sacrificed and no significant differences were observed in the incidence of hydrosalpinx in ASC KO, NLRP3 KO, and NLRC4 KO in comparison to their corresponding WT controls (Fig. 5A and B). Histopathological observations also showed no significant changes in the oviducts between the groups (data not shown). These data demonstrate that ASC KO mice display increased bacterial colonization just as IL-1R KO mice do, but do not show any reduction in oviduct pathology as observed for IL-1R KO (Fig 2A), compared to WT mice.

Inflammasome-independent IL-1β secretion in vivo during *C. muridarum* genital infection

In vitro infection data support a role for ASC inflammasome in IL-1β secretion (Fig 3B). However, during in vivo infection ASC KO mice do not display the reduction in pathology as observed in IL-1R KO or IL-1β KO mice (3). To understand this dichotomy, IL-1β levels in genital secretions of inflammasome KO mice were analyzed. IL-1β levels were dependent on ASC and NLRP3 only at day 2 postinfection, but independent of ASC or NLRP3 deficiency from day 3 to 10 postinfection (Fig 6A). In contrast, the secretion of another caspase-1 dependent protein IL-18 was completely dependent on ASC and was also reduced in NLRP3 KO mice compared to WT mice (Fig 6B), demonstrating that activation of caspase-1 is indeed compromised in these mice. These data demonstrate IL-1β production is independent of ASC inflammasome during genital infection and suggest that delayed infection clearance in ASC KO mice is likely to be independent of IL-1β levels and IL-1 signaling.

Decreased PMN recruitment during infection in IL-1R KO mice is associated with reduced pathology in IL-1R KO mice

To further understand the mechanism of differential oviduct pathology in IL-1R KO and inflammasome KO mice, recruitment of inflammastory cells to cervix, horns, and oviducts in IL-1R KO mice were tested at day 10 and day 20 postinfection. A fraction of the collagenase treated tissues were also analyzed for chlamydial burden by measuring IFU. Consistent with the data obtained from genital swabs (Fig 1A), IL-1R KO horns displayed increased bacterial colonization at both day 10 and day 20 postinfection, while the cervix showed increased IFU at day 10 post infection (Fig 7A and B). IL-1R KO oviducts showed equivalent levels of IFU as WT oviducts (Fig 7A and B), suggesting that the reduced incidence of hydrosalpinx at day 45 was not associated with decreased ascension of bacteria at early time points. Flow cytometric analysis showed a slight but significant increase in $CD45^+$ cells in IL-1R KO genital tracts (data not shown). When individual inflammatory cells were analyzed from the total live cell population, a large and significant decrease in the number of $Ly6G^+$ PMN was observed in IL-1R KO genital tracts in comparison to WT mice (Fig 7C and D). $CD4^+$ T cells were also significantly decreased in the oviducts at day 20 postinfection in the IL-1R KO mice (Fig 7E and F). In contrast, a significant increase in $F4/80^+$ macrophages (Fig 7G and H) was observed, which could account for the increased $CD45^+$ cells in IL-1R KO genital tracts. A similar decrease in $Ly6G^+$ PMN and $CD4^+$ T cells was observed within the CD45 population itself, indicating that there was no skewing of data due to changes in CD45 numbers between the two groups during infection. A representative oviduct sample from WT and IL-1R KO mice is shown (Fig 7I and J). The reduction in PMN numbers in IL-1R KO was due to lack of IL-1R signaling and not IL-1β

levels, since IL-1β levels in the genital secretions of IL-1R KO mice were comparable to WT mice (data not shown). Overall, the data indicates that absence of IL-1 signaling is associated with decreased PMN recruitment to the genital tracts despite increased infection. Importantly, this reduction in early PMN recruitment in IL-1R KO mice is associated with the decreased incidence of hydrosalpinx observed at day 45 postinfection in the oviducts (Fig 2A), consistent with the hypothesized role for neutrophils in ascending infection (31-33).

ASC KO mice display increased PMN recruitment and a significant role for ASC in T cell recruitment and function

Although ASC KO mice have prolonged infection like IL-1R KO, the pathological outcome of infection is unlike IL-1R KO. To investigate the cellular mechanism of increased infection and oviduct pathology in ASC KO mice, tissues from infected mice at days 10 and 20 postinfection were treated with collagenase and recruitment of inflammatory cells analyzed by flow cytometry. No difference in the overall numbers of $CD45^+$ cells were observed in all tissues between WT and ASC KO mice (data not shown). In contrast to IL-1R KO mice (Fig 7), increased numbers of PMN were observed at day 20 postinfection in ASC KO mice compared to WT mice (Fig 8A, B, E and F) in cervix and horn tissues. No significant differences in $F4/80^+$ macrophages populations were observed between the two groups at day 20 postinfection in the oviducts and horns, although some reduction was observed in ASC KO cervix at day 10 post infection (data not shown). However, a significant reduction in T cell recruitment to cervix, horns, and oviducts of ASC KO mice was observed compared to WT mice at day 20 postinfection (Fig 8C, B, E and F).

To further understand if the difference in T cell recruitment is reflective of the number of T cells in the iliac lymph nodes, iliac lymph nodes from WT and ASC KO mice were obtained at day 14 post infection. Surprisingly, there was a small but significant increase in the $CD3^+$ cells in the iliac lymph nodes of ASC KO mice compared to WT mice (data not shown). However, ASC KO T cells demonstrated a statistically significant decrease in chlamydial Ag-specific proliferation in comparison to cells isolated from WT mice (Fig 9A). Conversely, NLRP3 KO and NLRC4 KO T cells showed no decrease in T cell proliferation (data not shown). Culture supernatants from ASC KO T cells from both mitogen- and antigen-treated group showed reduced IFNγ and IL-17 (Fig 9B and C) suggesting a diminished Th1 and Th17 response in ASC KO mice. Overall, our data suggests that ASC KO mice show increased chlamydial colonization due to a T cell dysfunction and recruitment, despite normal IL-1β levels. Further, increased infection in ASC KO mice results in increased PMN recruitment, through an intact IL-1 signaling pathway, a potential explanation for the pathology observed in these mice.

Discussion

This study was undertaken to determine how caspase-1 is activated during genital chlamydial infection and its relationship to IL-1 signaling. Previous studies have shown that caspase-1 and the caspase-1 dependent cytokine IL-1β is associated with exacerbation of upper genital tract pathology during infection with *C. muridarum* (3, 8). In this study we

show that the absence of IL-1 signaling significantly protects oviducts from pathology during *C. muridarum* genital infection. This protection is observed despite increased chlamydial colonization, suggesting that IL-1 signaling is a double-edged sword with a beneficial effect for optimal infection clearance but also a deleterious effect by causing oviduct pathology during *C. muridarum* infection. The downstream effect of IL-1 signaling in host pathology is likely mediated through PMN recruitment to the genital tract, since lack of IL-1 signaling significantly reduced PMN infiltration into the genital tissue. These data are consistent with the important role for neutrophils in ascending infection (31-33). However, one cannot rule out additional cytopathic role for IL-1 signaling directly on epithelial cells as was shown using Fallopian tube organ culture (34). IL-1 signaling has also been shown to play a role in disrupting epithelial tight junction claudin-4 in a Rho-kinase dependent manner in gastric epithelial cells (35), suggesting additional mechanisms through which it could damage the oviduct epithelial cell junctions.

Inflammasome activation through NLRP3 and ASC is an essential step for IL-1β secretion during in vitro *C. trachomatis* infection (24, 25) and during *C. pneumoniae* lung infection (26). We speculate that during in vivo infection, macrophages and neutrophils coming to the site of infection can get prestimulated by various chlamydial TLR ligands. Therefore, it is critical to understand the components of inflammasome activation in pre-stimulated macrophages. Resting macrophages required ASC and NLRP3 for IL-1β secretion but occurred independent of NLRC4. However, in LPS-prestimulated macrophages, neither NLRP3 nor NLRC4 were required for IL-1β secretion following *C. muridarum* infection. Only loss of the adaptor protein ASC led to decreased secretion of IL-1β, suggesting that the crucial inflammasome in primed macrophages consists of caspase-1, ASC, and as of yet unidentified pyrin domain containing protein. AIM2, which responds to cytosolic DNA (22, 36, 37) and NALP1 (21) represent two possibilities. AIM2 is essential for inflammasome activation during *Streptococcus pneumoniae* infection (38), and could be the possible ASC-dependent inflammasome during chlamydial infection. The NALP1 possibility is also intriguing due to the fact that caspase-1 activation by *Bacillus anthracis* LeTx mediated by NALP1 (21) has the same potassium efflux and proteasome dependence (39-41) as chlamydial induced IL-1β secretion (3). Above and beyond NALP1 and AIM2, it is also likely there are inflammasomes that are yet to be discovered. It has been hypothesized that *Legionella pneumophila* can activate caspase-1 via ASC through an uncharacterized mechanism not involving NLRP3 or NLRC4 (42). Overall, the in vitro results in this study indicate that there are multiple inflammasomes activated by *C. muridarum* inside the cell depending on the cell status as shown for *L. monocytogenes* and *Yersinia pseudotuberculosis* (43, 44). With respect to chlamydial effectors inducing inflammasome activation, it has been speculated that chlamydial type III secretion (T3S) apparatus could be an important trigger for caspase-1 activation (3, 45). The fact that NLRC4 played no role might suggest otherwise, but it must be noted that NLRC4 appears to be activated only by flagellin or T3S rod proteins expressing a particular structural motif (18). It would be speculated that the chlamydial T3S rod protein also lacks this motif. Nevertheless, the absence of NLRC4 activation by *C. muridarum* does not conclude that T3S or T3S effectors are not important for caspase-1 activation.

Despite the critical role of ASC in IL-1β secretion during in vitro infection, during in vivo genital infection IL-1β secretion was dependent on ASC and NLRP3 only at day 2 postinfection. These data are reminiscent of in vitro findings in unstimulated macrophages. However, at all time points after day 2 postinfection, IL-1β secretion was independent of ASC and NLRP3. The caspase-1 activation was indeed ASC dependent as evidenced by decreased IL-18 levels in ASC KO mice. This dependency could imply that other inflammasome proteins, which do not require the adaptor ASC, could be compensating for the lack of NLRP3 and ASC to result in IL-1β secretion. The more likely interpretation of these results is that a substantial proportion of IL-1β produced during *C. muridarum* infection in the female genital tract is caspase-1 independent. Along similar lines, IL-1β expression during infection of mice with *Mycobacterium tuberculosis* was also found to occur in a caspase-1-independent fashion (47). Additionally, in mouse models of rheumatoid arthritis, it has been demonstrated that IL-1β from macrophages is caspase-1 dependent while neutrophil produced IL-1β is caspase-1 independent (48). Neutrophils possess serine proteases such as elastase and proteinase 3 that can accomplish the catalytic step of cleaving pro-IL-1β near the site where caspase-1 targets, processing the cytokine to its active form (49). We have shown that neutrophils isolated from genital tissue infected with *C. muridarum* have high expression of IL-1β (3). Consistent with the role of neutrophils for inflammasome-independent IL-1β production, ASC KO mice showed increased PMN recruitment and had significant IL-1β levels in their genital secretions. These data are in contrast to observed findings during *C. pneumoniae* infection in lungs where a direct correlation of IL-1 signaling, ASC KO, and NLRP3 KO was observed (26, 50). However, it must be noted that *C. pneumoniae* seems to be able to activate cytosolic sensors for other cytokine pathways in a manner different from *C. muridarum* (51-53). Therefore, drawing parallels between these two pathogens with respect to caspase-1 activation may not be precise.

Independent of IL-1β levels, ASC KO mice exhibited increased chlamydial colonization of *C. muridarum*. Additionally, infection course and pathology from ASC KO mice during genital chlamydial infection does not mirror the data from caspase-1 KO mice (8), which showed reduced oviduct pathology compared to WT mice. The phenotype in ASC KO could be attributed to decreased T cell function and recruitment to the genital tract. ASC is a cytosolic protein, to which an inflammatory role independent of caspase-1 and NLRP3 has been demonstrated in an antigen-induced arthritis model (54). Using the same model, it was shown that ASC KO T cells show decreased cellular proliferation (54) and diminished priming from DCs (56). In a mouse model for experimental autoimmune encephalomyelitis, ASC deficient CD4 T cell exhibited impaired survival (55), illustrating another example where ASC seems to be able to play a crucial caspase-1 independent role. Recently, it has been demonstrated that ASC controlled mRNA stability of Dock2, a guanine nucleotide exchange factor which mediates Rac-dependent signaling in immune cells affecting T cell migration and antigen uptake by DC, in an inflammasome-independent manner (57). Therefore, during in vivo chlamydial infection, we propose that antigen specific T cells are likely exhibiting impaired survival and decreased proliferation in the absence of ASC, resulting in delayed infection clearance.

Overall, we further our studies with IL-1β KO mice (3) and provide a conclusive role for IL-1 signaling in progression of oviduct pathology. The protection from oviduct pathology in IL-1R KO mice is particularly striking as these mice have increased chlamydial burden. These results suggest IL-1R signaling to be a major host cytokine signaling pathway contributing directly to oviduct pathology. However, inflammasome activation in vivo is not a major contributor to IL-1β levels during in vivo infection, although ASC has a specific role in T cell function and activation necessary for resolving infection. It remains to be determined how IL-1β is produced during in vivo infection and if modulating this pathway by antagonists can prevent oviduct pathology during infection.

Acknowledgments

NLRP3 KO, NLRC4 KO, and ASC KO mice were kindly provided by Genentech Inc. (Dr. V. Dixit). Thanks to Shanmugam Nagarajan (University of Pittsburgh) and John Gregan (ACHRI) for critical and editorial comments on the manuscript.

References

1. Mardh PA. Tubal factor infertility, with special regard to chlamydial salpingitis. Curr Opin Infect Dis. 2004; 17:49–52. [PubMed: 15090891]
2. Darville T, O'Neill JM, Andrews CW Jr, Nagarajan UM, Stahl L, Ojcius DM. Toll-like receptor-2, but not Toll-like receptor-4, is essential for development of oviduct pathology in chlamydial genital tract infection. J Immunol. 2003; 171:6187–6197. [PubMed: 14634135]
3. Prantner D, Darville T, Sikes JD, Andrews CW Jr, Brade H, Rank RG, Nagarajan UM. Critical role for interleukin-1beta (IL-1beta) during Chlamydia muridarum genital infection and bacterial replication-independent secretion of IL-1beta in mouse macrophages. Infect Immun. 2009; 77:5334–5346. [PubMed: 19805535]
4. Kuno K, Matsushima K. The IL-1 receptor signaling pathway. Journal of leukocyte biology. 1994; 56:542–547. [PubMed: 7964161]
5. Hannum CH, Wilcox CJ, Arend WP, Joslin FG, Dripps DJ, Heimdal PL, Armes LG, Sommer A, Eisenberg SP, Thompson RC. Interleukin-1 receptor antagonist activity of a human interleukin-1 inhibitor. Nature. 1990; 343:336–340. [PubMed: 2137200]
6. Thornberry NA, Bull HG, Calaycay JR, Chapman KT, Howard AD, Kostura MJ, Miller DK, Molineaux SM, Weidner JR, Aunins J, et al. A novel heterodimeric cysteine protease is required for interleukin-1 beta processing in monocytes. Nature. 1992; 356:768–774. [PubMed: 1574116]
7. Ghayur T, Banerjee S, Hugunin M, Butler D, Herzog L, Carter A, Quintal L, Sekut L, Talanian R, Paskind M, Wong W, Kamen R, Tracey D, Allen H. Caspase-1 processes IFN-gamma-inducing factor and regulates LPS-induced IFN-gamma production. Nature. 1997; 386:619–623. [PubMed: 9121587]
8. Cheng W, Shivshankar P, Li Z, Chen L, Yeh IT, Zhong G. Caspase-1 contributes to Chlamydia trachomatis-induced upper urogenital tract inflammatory pathologies without affecting the course of infection. Infect Immun. 2008; 76:515–522. [PubMed: 18025098]
9. Martinon F, Burns K, Tschopp J. The inflammasome: a molecular platform triggering activation of inflammatory caspases and processing of proIL-beta. Mol Cell. 2002; 10:417–426. [PubMed: 12191486]
10. Miao EA, Ernst RK, Dors M, Mao DP, Aderem A. Pseudomonas aeruginosa activates caspase 1 through Ipaf. Proc Natl Acad Sci U S A. 2008; 105:2562–2567. [PubMed: 18256184]
11. Suzuki T, Franchi L, Toma C, Ashida H, Ogawa M, Yoshikawa Y, Mimuro H, Inohara N, Sasakawa C, Nunez G. Differential regulation of caspase-1 activation, pyroptosis, and autophagy via Ipaf and ASC in Shigella-infected macrophages. PLoS Pathog. 2007; 3:e111. [PubMed: 17696608]

12. Amer A, Franchi L, Kanneganti TD, Body-Malapel M, Ozoren N, Brady G, Meshinchi S, Jagirdar R, Gewirtz A, Akira S, Nunez G. Regulation of Legionella phagosome maturation and infection through flagellin and host Ipaf. J Biol Chem. 2006; 281:35217–35223. [PubMed: 16984919]
13. Mariathasan S, Weiss DS, Newton K, McBride J, O'Rourke K, Roose-Girma M, Lee WP, Weinrauch Y, Monack DM, Dixit VM. Cryopyrin activates the inflammasome in response to toxins and ATP. Nature. 2006; 440:228–232. [PubMed: 16407890]
14. Masumoto J, Taniguchi S, Ayukawa K, Sarvotham H, Kishino T, Niikawa N, Hidaka E, Katsuyama T, Higuchi T, Sagara J. ASC, a novel 22-kDa protein, aggregates during apoptosis of human promyelocytic leukemia HL-60 cells. J Biol Chem. 1999; 274:33835–33838. [PubMed: 10567338]
15. Srinivasula SM, Poyet JL, Razmara M, Datta P, Zhang Z, Alnemri ES. The PYRIN-CARD Protein ASC Is an Activating Adaptor for Caspase-1. Journal of Biological Chemistry. 2002; 277:21119–21122. [PubMed: 11967258]
16. Halle A, Hornung V, Petzold GC, Stewart CR, Monks BG, Reinheckel T, Fitzgerald KA, Latz E, Moore KJ, Golenbock DT. The NALP3 inflammasome is involved in the innate immune response to amyloid-beta. Nat Immunol. 2008; 9:857–865. [PubMed: 18604209]
17. Martinon F, Petrilli V, Mayor A, Tardivel A, Tschopp J. Gout-associated uric acid crystals activate the NALP3 inflammasome. Nature. 2006; 440:237–241. [PubMed: 16407889]
18. Miao EA, Mao DP, Yudkovsky N, Bonneau R, Lorang CG, Warren SE, Leaf IA, Aderem A. Innate immune detection of the type III secretion apparatus through the NLRC4 inflammasome. Proc Natl Acad Sci U S A. 2010; 107:3076–3080. [PubMed: 20133635]
19. Kofoed EM, Vance RE. Innate immune recognition of bacterial ligands by NAIPs determines inflammasome specificity. Nature. 2011; 477:592–595. [PubMed: 21874021]
20. Zhao Y, Yang J, Shi J, Gong YN, Lu Q, Xu H, Liu L, Shao F. The NLRC4 inflammasome receptors for bacterial flagellin and type III secretion apparatus. Nature. 2011; 477:596–600. [PubMed: 21918512]
21. Boyden ED, Dietrich WF. Nalp1b controls mouse macrophage susceptibility to anthrax lethal toxin. Nat Genet. 2006; 38:240–244. [PubMed: 16429160]
22. Hornung V, Ablasser A, Charrel-Dennis M, Bauernfeind F, Horvath G, Caffrey DR, Latz E, Fitzgerald KA. AIM2 recognizes cytosolic dsDNA and forms a caspase-1-activating inflammasome with ASC. Nature. 2009; 458:514–518. [PubMed: 19158675]
23. Rathinam VA, Jiang Z, Waggoner SN, Sharma S, Cole LE, Waggoner L, Vanaja SK, Monks BG, Ganesan S, Latz E, Hornung V, Vogel SN, Szomolanyi-Tsuda E, Fitzgerald KA. The AIM2 inflammasome is essential for host defense against cytosolic bacteria and DNA viruses. Nat Immunol. 2010; 11:395–402. [PubMed: 20351692]
24. Abdul-Sater AA, Koo E, Hacker G, Ojcius DM. Inflammasome-dependent caspase-1 activation in cervical epithelial cells stimulates growth of the intracellular pathogen Chlamydia trachomatis. J Biol Chem. 2009; 284:26789–26796. [PubMed: 19648107]
25. Abdul-Sater AA, Said-Sadier N, Padilla EV, Ojcius DM. Chlamydial infection of monocytes stimulates IL-1beta secretion through activation of the NLRP3 inflammasome. Microbes Infect. 2010; 12:652–661. [PubMed: 20434582]
26. He X, Mekasha S, Mavrogiorgos N, Fitzgerald KA, Lien E, Ingalls RR. Inflammation and fibrosis during Chlamydia pneumoniae infection is regulated by IL-1 and the NLRP3/ASC inflammasome. J Immunol. 2010; 184:5743–5754. [PubMed: 20393140]
27. Mariathasan S, Newton K, Monack DM, Vucic D, French DM, Lee WP, Roose-Girma M, Erickson S, Dixit VM. Differential activation of the inflammasome by caspase-1 adaptors ASC and Ipaf. Nature. 2004; 430:213–218. [PubMed: 15190255]
28. Nagarajan UM, Ojcius DM, Stahl L, Rank RG, Darville T. Chlamydia trachomatis induces expression of IFN-gamma-inducible protein 10 and IFN-beta independent of TLR2 and TLR4, but largely dependent on MyD88. J Immunol. 2005; 175:450–460. [PubMed: 15972679]
29. Caldwell HD, Kromhout J, Schachter J. Purification and partial characterization of the major outer membrane protein of Chlamydia trachomatis. Infect Immun. 1981; 31:1161–1176. [PubMed: 7228399]

30. Horai R, Asano M, Sudo K, Kanuka H, Suzuki M, Nishihara M, Takahashi M, Iwakura Y. Production of mice deficient in genes for interleukin (IL)-1alpha, IL-1beta, IL-1alpha/beta, and IL-1 receptor antagonist shows that IL-1beta is crucial in turpentine-induced fever development and glucocorticoid secretion. The Journal of experimental medicine. 1998; 187:1463–1475. [PubMed: 9565638]

31. Lee HY, Schripsema JH, Sigar IM, Lacy SR, Kasimos JN, Murray CM, Ramsey KH. A role for CXC chemokine receptor-2 in the pathogenesis of urogenital Chlamydia muridarum infection in mice. FEMS Immunol Med Microbiol. 2010; 60:49–56. [PubMed: 20602634]

32. Lee HY, Schripsema JH, Sigar IM, Murray CM, Lacy SR, Ramsey KH. A link between neutrophils and chronic disease manifestations of Chlamydia muridarum urogenital infection of mice. FEMS Immunol Med Microbiol. 2010; 59:108–116. [PubMed: 20370824]

33. Rank RG, Whittimore J, Bowlin AK, Wyrick PB. In Vivo Ultrastructural Analysis of the Intimate Relationship between Polymorphonuclear Leukocytes and the Chlamydial Developmental Cycle. Infect Immun. 2011; 79:3291–3301. [PubMed: 21576327]

34. Hvid M, Baczynska A, Deleuran B, Fedder J, Knudsen HJ, Christiansen G, Birkelund S. Interleukin-1 is the initiator of Fallopian tube destruction during Chlamydia trachomatis infection. Cell Microbiol. 2007; 9:2795–2803. [PubMed: 17614966]

35. Lapointe TK, O'Connor PM, Jones NL, Menard D, Buret AG. Interleukin-1 receptor phosphorylation activates Rho kinase to disrupt human gastric tight junctional claudin-4 during Helicobacter pylori infection. Cellular microbiology. 2010; 12:692–703. [PubMed: 20070312]

36. Burckstummer T, Baumann C, Bluml S, Dixit E, Durnberger G, Jahn H, Planyavsky M, Bilban M, Colinge J, Bennett KL, Superti-Furga G. An orthogonal proteomic-genomic screen identifies AIM2 as a cytoplasmic DNA sensor for the inflammasome. Nature immunology. 2009; 10:266–272. [PubMed: 19158679]

37. Fernandes-Alnemri T, Yu JW, Datta P, Wu J, Alnemri ES. AIM2 activates the inflammasome and cell death in response to cytoplasmic DNA. Nature. 2009; 458:509–513. [PubMed: 19158676]

38. Fang R, Tsuchiya K, Kawamura I, Shen Y, Hara H, Sakai S, Yamamoto T, Fernandes-Alnemri T, Yang R, Hernandez-Cuellar E, Dewamitta SR, Xu Y, Qu H, Alnemri ES, Mitsuyama M. Critical Roles of ASC Inflammasomes in Caspase-1 Activation and Host Innate Resistance to Streptococcus pneumoniae Infection. Journal of immunology. 2011; 187:4890–4899.

39. Wickliffe KE, Leppla SH, Moayeri M. Anthrax lethal toxin-induced inflammasome formation and caspase-1 activation are late events dependent on ion fluxes and the proteasome. Cell Microbiol. 2008; 10:332–343. [PubMed: 17850338]

40. Squires RC, Muehlbauer SM, Brojatsch J. Proteasomes control caspase-1 activation in anthrax lethal toxin-mediated cell killing. J Biol Chem. 2007; 282:34260–34267. [PubMed: 17878154]

41. Fink SL, Bergsbaken T, Cookson BT. Anthrax lethal toxin and Salmonella elicit the common cell death pathway of caspase-1-dependent pyroptosis via distinct mechanisms. Proc Natl Acad Sci U S A. 2008; 105:4312–4317. [PubMed: 18337499]

42. Case CL, Shin S, Roy CR. Asc and Ipaf Inflammasomes direct distinct pathways for caspase-1 activation in response to Legionella pneumophila. Infection and immunity. 2009; 77:1981–1991. [PubMed: 19237518]

43. Warren SE, Mao DP, Rodriguez AE, Miao EA, Aderem A. Multiple Nod-like receptors activate caspase 1 during Listeria monocytogenes infection. J Immunol. 2008; 180:7558–7564. [PubMed: 18490757]

44. Brodsky IE, Palm NW, Sadanand S, Ryndak MB, Sutterwala FS, Flavell RA, Bliska JB, Medzhitov R. A Yersinia effector protein promotes virulence by preventing inflammasome recognition of the type III secretion system. Cell host & microbe. 2010; 7:376–387. [PubMed: 20478539]

45. Wolf K, Betts HJ, Chellas-Gery B, Hower S, Linton CN, Fields KA. Treatment of Chlamydia trachomatis with a small molecule inhibitor of the Yersinia type III secretion system disrupts progression of the chlamydial developmental cycle. Mol Microbiol. 2006; 61:1543–1555. [PubMed: 16968227]

46. Lilo S, Zheng Y, Bliska JB. Caspase-1 activation in macrophages infected with Yersinia pestis KIM requires the type III secretion system effector YopJ. Infect Immun. 2008; 76:3911–3923. [PubMed: 18559430]
47. Mayer-Barber KD, Barber DL, Shenderov K, White SD, Wilson MS, Cheever A, Kugler D, Hieny S, Caspar P, Nunez G, Schlueter D, Flavell RA, Sutterwala FS, Sher A. Caspase-1 independent IL-1beta production is critical for host resistance to mycobacterium tuberculosis and does not require TLR signaling in vivo. Journal of immunology. 2010; 184:3326–3330.
48. Joosten LA, Netea MG, Fantuzzi G, Koenders MI, Helsen MM, Sparrer H, Pham CT, van der Meer JW, Dinarello CA, van den Berg WB. Inflammatory arthritis in caspase 1 gene-deficient mice: contribution of proteinase 3 to caspase 1-independent production of bioactive interleukin-1beta. Arthritis and rheumatism. 2009; 60:3651–3662. [PubMed: 19950280]
49. Coeshott C, Ohnemus C, Pilyavskaya A, Ross S, Wieczorek M, Kroona H, Leimer AH, Cheronis J. Converting enzyme-independent release of tumor necrosis factor alpha and IL-1beta from a stimulated human monocytic cell line in the presence of activated neutrophils or purified proteinase 3. Proc Natl Acad Sci U S A. 1999; 96:6261–6266. [PubMed: 10339575]
50. Shimada K, Crother TR, Karlin J, Chen S, Chiba N, Ramanujan VK, Vergnes L, Ojcius DM, Arditi M. Caspase-1 dependent IL-1beta secretion is critical for host defense in a mouse model of Chlamydia pneumoniae lung infection. PloS one. 2011; 6:e21477. [PubMed: 21731762]
51. Buss C, Opitz B, Hocke AC, Lippmann J, van Laak V, Hippenstiel S, Krull M, Suttorp N, Eitel J. Essential role of mitochondrial antiviral signaling, IFN regulatory factor (IRF)3, and IRF7 in Chlamydophila pneumoniae-mediated IFN-beta response and control of bacterial replication in human endothelial cells. J Immunol. 2010; 184:3072–3078. [PubMed: 20154210]
52. Chiliveru S, Birkelund S, Paludan SR. Induction of interferon-stimulated genes by Chlamydia pneumoniae in fibroblasts is mediated by intracellular nucleotide-sensing receptors. PLoS One. 2010; 5:e10005. [PubMed: 20386592]
53. Prantner D, Darville T, Nagarajan UM. Stimulator of IFN gene is critical for induction of IFN-beta during Chlamydia muridarum infection. J Immunol. 2010; 184:2551–2560. [PubMed: 20107183]
54. Kolly L, Karababa M, Joosten LA, Narayan S, Salvi R, Petrilli V, Tschopp J, van den Berg WB, So AK, Busso N. Inflammatory role of ASC in antigen-induced arthritis is independent of caspase-1, NALP-3, and IPAF. J Immunol. 2009; 183:4003–4012. [PubMed: 19717512]
55. Shaw PJ, Lukens JR, Burns S, Chi H, McGargill MA, Kanneganti TD. Cutting edge: critical role for PYCARD/ASC in the development of experimental autoimmune encephalomyelitis. Journal of immunology. 2010; 184:4610–4614.
56. Ippagunta SK, Brand DD, Luo J, Boyd KL, Calabrese C, Stienstra R, Van de Veerdonk FL, Netea MG, Joosten LA, Lamkanfi M, Kanneganti TD. Inflammasome-independent role of apoptosis-associated speck-like protein containing a CARD (ASC) in T cell priming is critical for collagen-induced arthritis. The Journal of biological chemistry. 2010; 285:12454–12462. [PubMed: 20177071]
57. Ippagunta SK, Malireddi RK, Shaw PJ, Neale GA, Walle LV, Green DR, Fukui Y, Lamkanfi M, Kanneganti TD. The inflammasome adaptor ASC regulates the function of adaptive immune cells by controlling Dock2-mediated Rac activation and actin polymerization. Nature immunology. 2011; 12:1010–1016. [PubMed: 21892172]

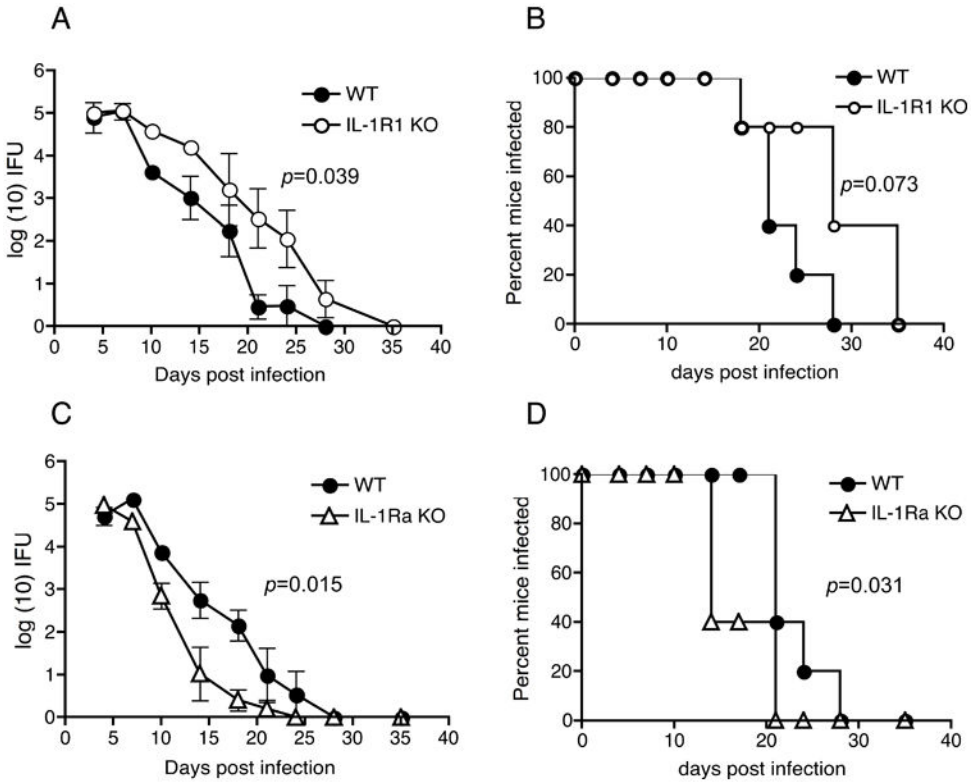

Figure 1. IL-1R deficiency results in enhanced chlamydial colonization while the deficiency of its antagonist IL-Ra reduces bacterial colonization and augments infection clearance during genital *C. muridarum* infection

C. muridarum infection course in *(A)*, WT (N=5) and IL-1R KO (N=5), and *(C)*, WT (N=5) and IL-1Ra KO (N=5) mice. Log_{10} (IFUs/ml) were calculated from genital swabs as described in Methods and graphed as means ± standard error of the means of animals positive for infection on that day. Significance was determined by two-way RM ANOVA (WT vs. IL-1R KO: $p = 0.039$; WT vs. IL-Ra KO: $p = 0.015$ *(A)*. Percent of mice that remain infected in each group are indicated in *(B)* and *(D)*. $P = 0.0737$ for WT vs. IL-1R KO *(B)* and $p = 0.0311$ for WT vs. IL-1Ra KO *(D)* by Kaplan-Meier survival analysis. A representative of 4 experiments for *(A)* and *(B)* and of 2 experiments for *(C)* and *(D)* is shown.

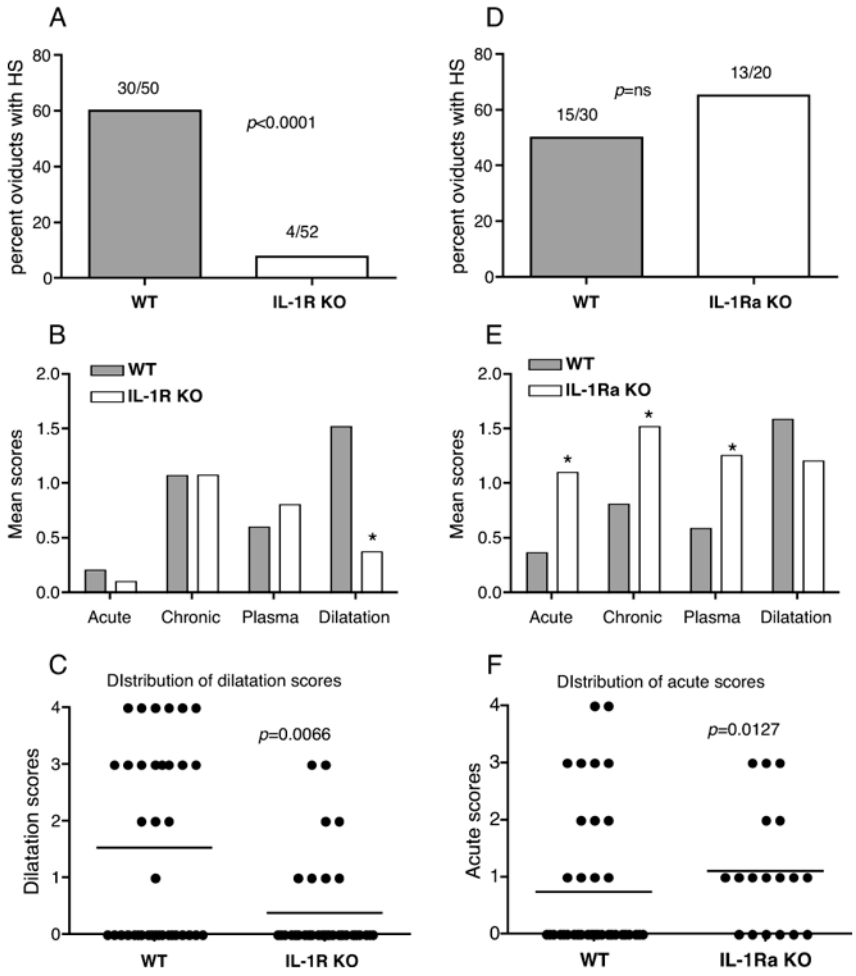

Figure 2. IL-R KO mice display reduced incidence of hydrosalpinx and histopathological dilatation of the oviducts, while IL-1Ra KO oviducts have increased inflammation

Percentage of oviducts developing hydrosalpinx in WT and IL-1R-KO mice *(A)*, and WT and IL-1Ra KO mice *(D)*. Actual numbers of hydrosalpinx from the total oviduct numbers are represented over the bars. Significance determined by Fisher's exact test. Mean scores from histopathology scoring for WT vs. IL-1R KO *(B)* and WT vs. IL-1Ra KO *(E)* in each category PMN (acute), mononuclear cells (chronic), plasma cells, and dilatation are indicated. An asterisk denotes a statistically significant difference ($p<0.05$) between the two groups using Mann Whitney test. The grades were classified as 1; very little, 2; mild, 3; moderate, and 4; severe. Distribution of dilatation or acute scores for individual oviducts in (*B* and *E)* are shown by plotting dilatation scores *(C)* for WT and IL-1R KO mice and acute cells score *(F)* for WT vs. IL-1Ra KO mice. Pathology scores are data combined from 4 independent experiments for WT vs. IL-1R KO (N=25 WT and N=26 IL-1R KO mice) and 2 experiments for WT vs. IL-1Ra KO (N=15 WT and N=10 IL-1Ra KO mice).

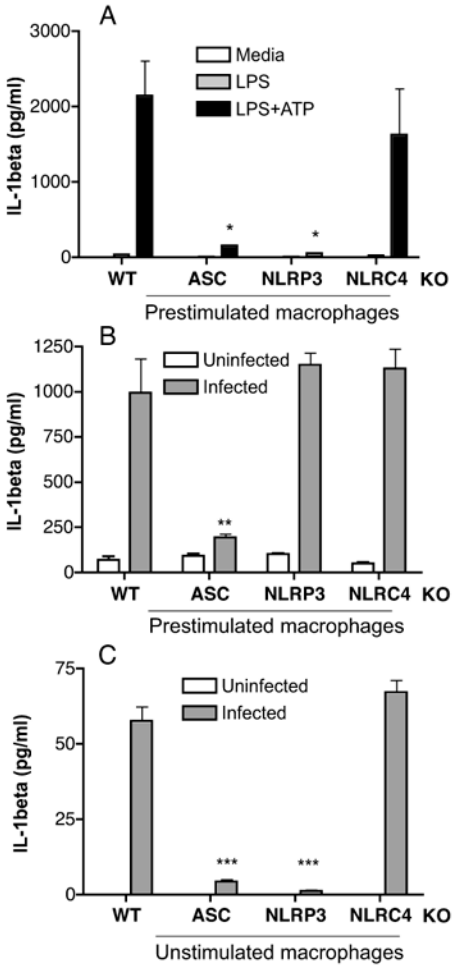

Figure 3. IL-1β secretion in prestimulated macrophages is NLRP3-independent, but ASC-dependent

Mouse peritoneal macrophages (8×10^5/well) from WT, ASC KO, NLRP3 KO, and NLRC4 KO mice were prestimulated with *E.coli* LPS for 6 h, followed by ATP stimulation for 30 min *(A)* or infected with *C. muridarum* at 1MOI *(B)*. Unstimulated macrophages were infected with *C. muridarum (C)*. Culture supernatants were analyzed for IL-1β by ELISA. Data represents IL-1β levels measured by ELISA in supernatant collected 2 h after stimulation *(A)* or 18 h postinfection *(B)* and *(C)*. Significance determined by one-way ANOVA, where * is $p<0.05$, ** is $p<0.01$, and *** is $p<0.001$. A representative of 4 experiments is shown.

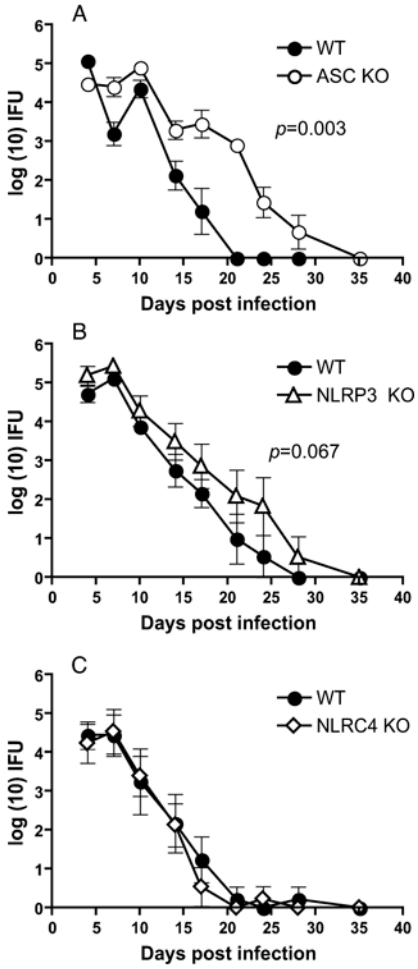

Figure 4. ASC deficiency significantly increases bacterial colonization and delays genital *C. muridarum* infection clearance, while NLRP3 has a marginal effect and NLRC4 deficiency has no effect

C. muridarum infection course in *(A)* WT (N=5) and ASC KO (N=5), *(B)* WT (N=5) and NLRP3 KO (N=5) mice, and *(C)*, WT (N=10) and NLRP3 KO (N=10) mice. Log_{10} (IFUs/ml) were calculated from genital swabs as described in Methods and graphed as means ± standard error of the means for animals positive for infection on that day. Significance was determined by two-way RM ANOVA (WT vs. ASC KO, p =0.003; WT vs. NLRP3 KO, $p < 0.067$). Kaplan-Meier survival analysis showed a significance of p= 0.005 for WT vs. ASC KO mice clearing infection. A representative of 3 experiments is shown.

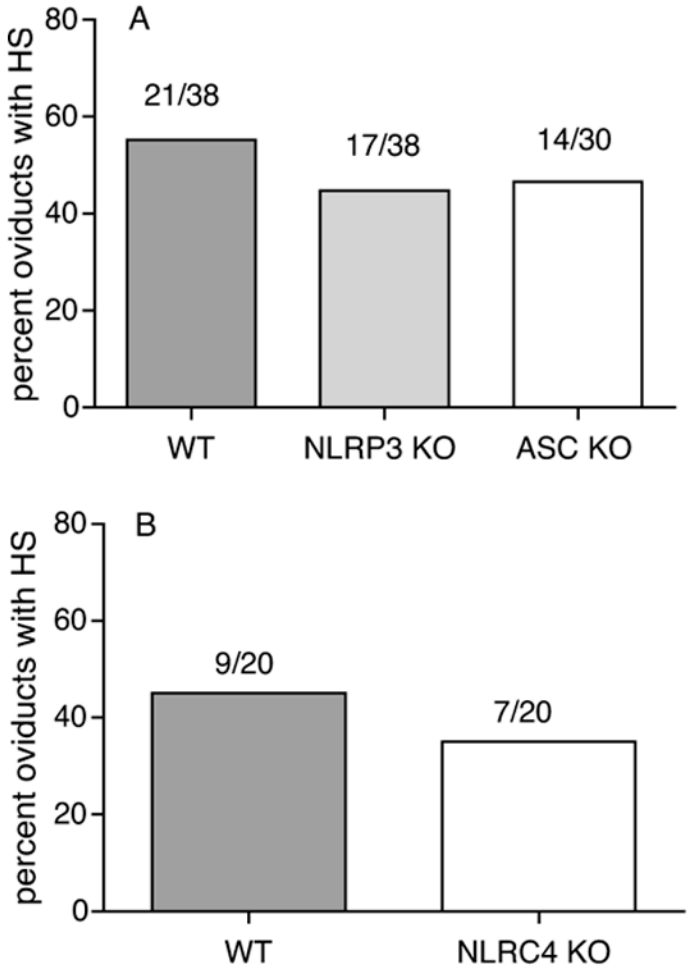

Figure 5. ASC KO, NLRP3 KO and NLRC4 display similar incidence of oviduct hydrosalpinx as WT mice

Percentage of oviducts developing hydrosalpinx in WT, ASC KO, NLRP3 KO *(A)*, and NLRC4 KO *(B)*. Actual numbers of hydrosalpinx from the total oviduct numbers are represented over the bars. Data for WT vs ASC KO and NLRP3KO are combined data from 3 independent experiments.

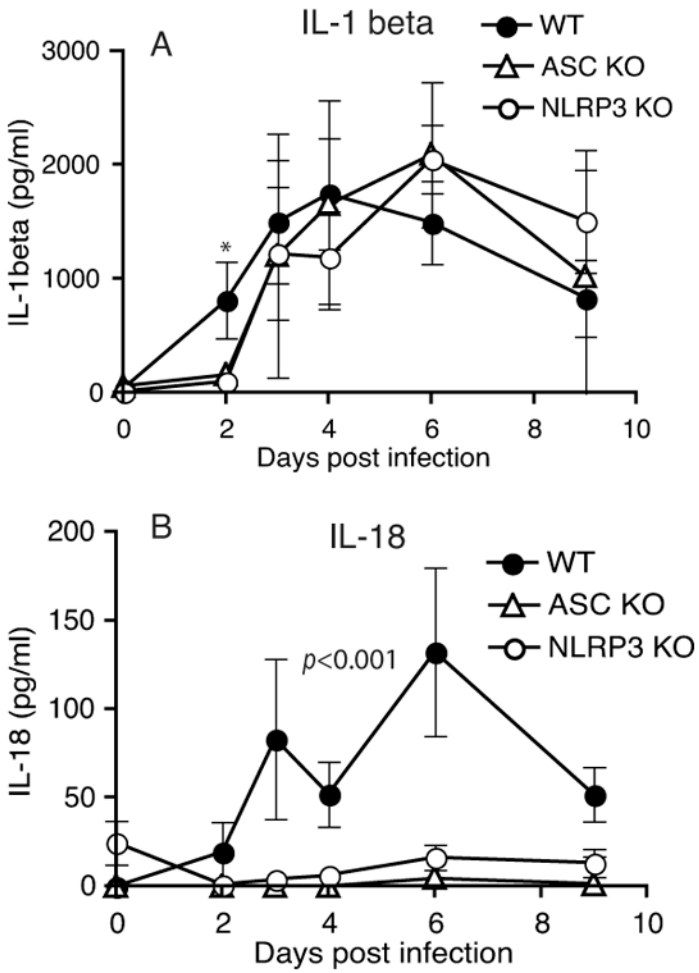

Figure 6. IL-1β levels in genital secretion of ASC and NLRP3 KO mice are comparable to WT mice, but IL-18 levels are significantly reduced

Genital secretions collected using sponges on infected mice were eluted and analyzed for IL-1β *(A)* and IL-18 *(B)* by ELISA. *P*<0.001 by two-way ANOVA for WT vs. NLRP3 KO and WT vs. ASC- IL-18 levels. An asterisk indicates significant change (p<0.05) for that specific time point.

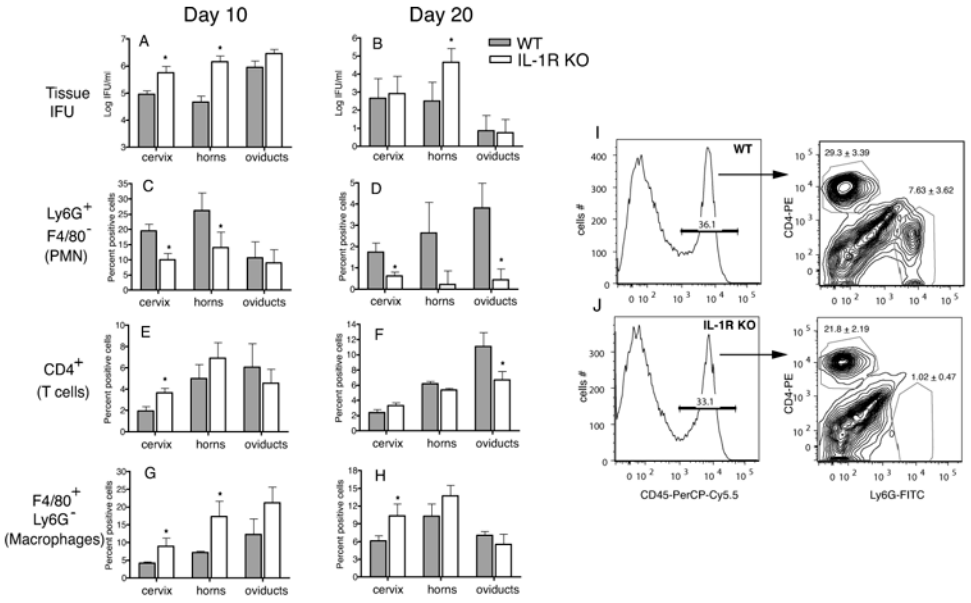

Figure 7. IL-1R KO genital tissues display a reduced number of PMN, despite increased bacterial burden

WT (N=5) and IL-1R KO (N=5) mice were infected with 1×10^6 IFU and cervix, horns, and oviduct tissue processed at day 10 and day 20 postinfection as described in Methods for IFU (*A* and *B*) and flow cytometry. Total live cells were analyzed $CD45^+$ $Ly6G^+$ $F4/80^-$ (PMN) (*C* and *D*), $CD45^+$ $CD4^+$ (CD4 T cells) (*E* and *F*), and $CD45^+$ $Ly6G^-$ $F4/80^+$ (macrophages) (*G* and *H*). A representative of 2 experiments is shown. An asterisk represents $p<0.05$ by unpaired T test between WT and KO for each tissue. A histogram and contour plot of a representative oviduct sample at day 20 postinfection from WT and IL-1R KO mice is shown (*I* and *J*). Cells were gated for $CD45^+$ cells before analyzing numbers of PMN and CD4 T cells. Numbers represent an average from 5 mice for each group. P=0.003 ($CD4^+$ T cells) and P=0.004 ($Ly6G^+$PMN) by unpaired T test.

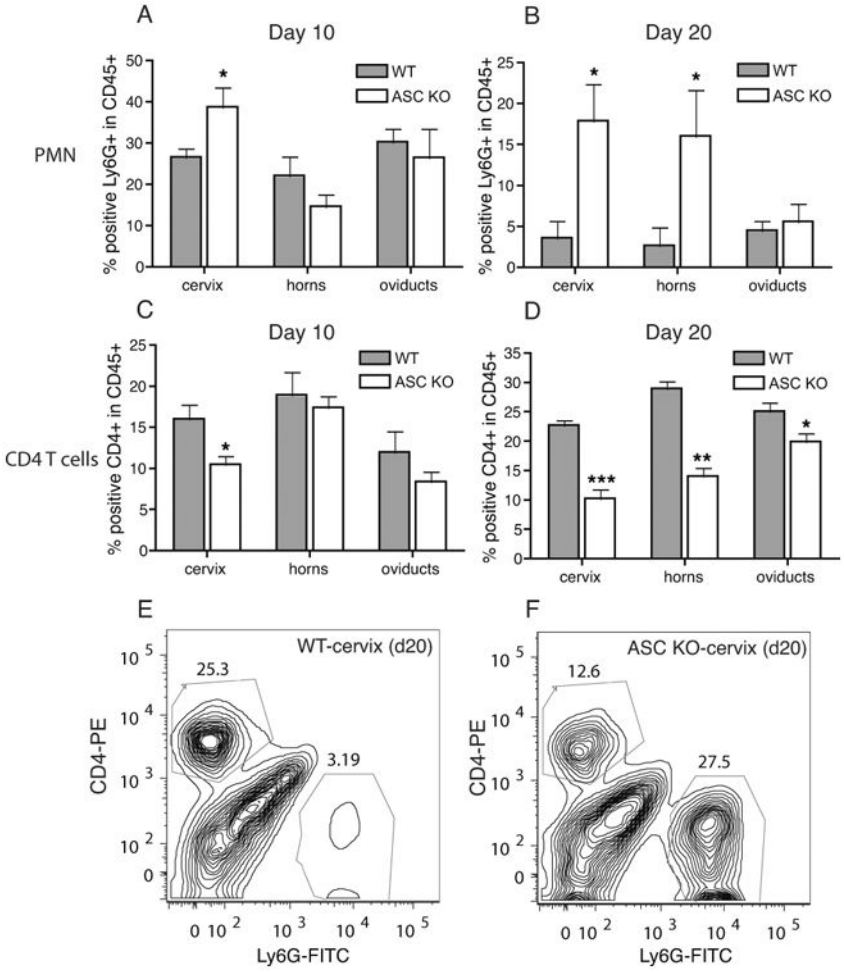

Figure 8. ASC KO mice have significantly reduced CD4 T cell but increased PMN recruitment to the genital tract

Cervix, horns, and oviducts from day 10 and day 20 postinfection (WT, N=5, and ASC KO, N=5) were analyzed for Ly6G+ PMNs (*A* and *B*) or $CD4^+$ T cells (*C* and *D*), within the live $CD45^+$ population. * indicates $p<0.05$, ** $p<0.01$, and *** $p<0.001$ by unpaired student T test. A representative contour plot of cervix samples from WT (*E*) and ASC KO (*F*) at day 20 postinfection is shown.

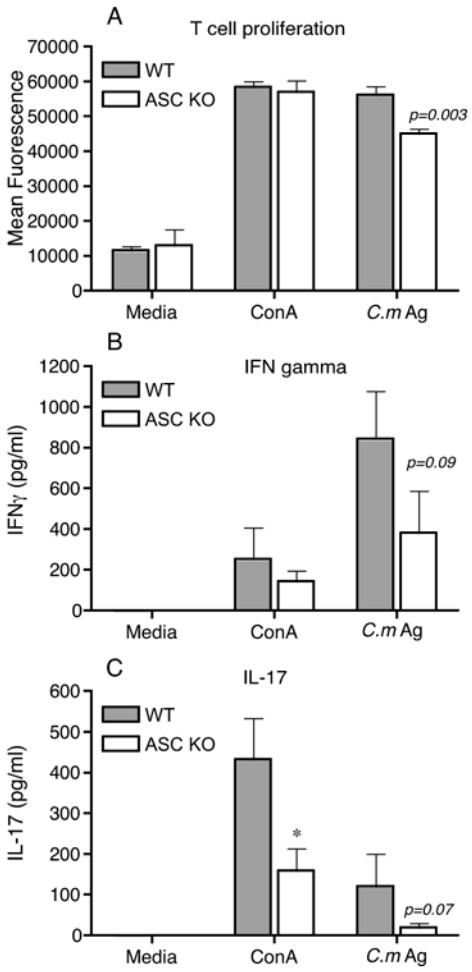

Figure 9. ASC KO T cells show reduced chlamydial-specific proliferation and IFNγ and IL-17 production

WT (N=4) and ASC KO (N=5) mice were infected with *C. muridarum* and iliac nodes harvested at day 14 postinfection. Cells were processed for *C. muridarum*-antigen (*C.m* Ag) - or mitogen (concanavalin A)-specific T cell proliferation (ConA) as described in Methods. After 4 days, alamarBlue™ was added and fluorescence measured after 24 h (*A*). Each sample was set in triplicate and data shows average for all mice in each group and SEM. Supernatants from T cell proliferation were analyzed for IFNγ at 1:10 dilution (*B*) or directly for IL-17 by ELISA (*C*). Significance measured using unpaired T test and * indicates $p<0.05$.